ORIGINAL ARTICLE

Multi-target potential of *moringa oleifera*-derived compounds against cariogenic and endodontic virulence proteins revealed by molecular docking: an in *silico* experimental study

Meiny Faudah Amin[1*]
Dikdik Kurnia[2]
Taufiq Ariwibowo[1]
Dicky Hardi[1]

[1]Department Conservative Dentistry, Faculty of Dentistry, Universitas Trisakti
Jakarta Barat, Indonesia
[2] Department of Chemistry, Faculty of Mathematics, and Natural Sciences, Universitas Padjadjaran
Sumedang, Indonesia

* Correspondence:
meiny.faudah@trisakti.ac.id

Received: 27 January 2026
Revised: 26 Februari 2026
Accepted: 20 March 2026
Published: 31 March 2026
DOI:10.24198/pjd.vol38no1.68102

p-ISSN 1979-0201
e-ISSN 2549-6212

Citation:
Amin, MF, Kurnia, D, Ariwibowo,T, Hardi, D. Multi-target potential of moringa oleifera-derived compounds against cariogenic and endodontic virulence proteins revealed by molecular docking: an in silico experimental study. Padjadjaran J. Dent, March. 2026; 38(1): 142-154.

ABSTRACT

Introduction: Dental infections are multifactorial diseases involving bacterial biofilms and host immune responses. Natural compounds with antibacterial activity, such as *Moringa oleifera*, have been explored as alternatives to conventional antibiotics. This study aimed to evaluate the interaction profiles of four Moringa oleifera–derived compounds against multiple virulence-associated proteins of cariogenic and endodontic pathogens using in silico molecular docking. **Methods**: This study was an in silico experimental study using molecular docking simulations to evaluate the binding energy of four *M. oleifera*-derived compounds (eugenol, trans-anethole, arachidonic acid, and phytosphingosine) with five key virulence-associated proteins of cariogenic and endodontic pathogens (Cystalysin, SrpA, FimA, RadD, and Ddl). AutoDock 4.0 was used for the docking simulations. Docking results were analyzed based on binding energy (ΔG) and inhibition constant (Ki) values. The best binding conformations were selected according to the lowest binding energy and visualized to identify key ligand–protein interactions using Discovery Studio Visualizer. **Results**: The phytosphingosine-Ddl exhibited the lowest binding energy of -7.42 kcal/mol, followed by eugenol with three different receptors (Cystalysin, SrpA, and FimA) and arachidonic acid-RadD. The lowest inhibition constant was shown by the phytosphingosine-Ddl complex at 3.61 μM. Each compound interacted with various targets, but phytosphingosine exhibited the most consistent and widespread predicted binding via hydrogen bonds with Glu222, Arg291, Glu306, Asp293, Lys251, and hydrophobic interactions of Phe295, Phe245, Phe175, and Leu145. **Conclusion:** This in silico molecular docking study demonstrated that *Moringa oleifera*–derived compounds, particularly phytosphingosine, exhibit strong binding affinity toward key virulence-associated proteins of cariogenic and endodontic pathogens. These findings highlight the potential of *M. oleifera* as a natural source of antibacterial agents and support further experimental validation of its therapeutic applications in oral infections.

KEYWORDS

Molecular docking, *moringa oleifera*, dental caries, cariogenic bacteria, virulence factors

INTRODUCTION

Various dental diseases in conservative dentistry, including cariogenic and endodontic infections, are inflammatory conditions caused by infection that affects both hard and soft dental tissues, such as enamel, dentin, pulp, and periapical tissues.[1] Furthermore, disease development, susceptibility, and progression are influenced by genetic, environmental, and behavioral factors. Multiple factors

contribute to the aetiology of periodontitis.[2] In a vulnerable host, subgingival dental biofilm triggers an inflammatory and immunological reaction that ultimately results in the irreversible destruction from dental tissue to the periodontium, which includes the alveolar bone and periodontal ligament.[3]

Subgingival bacteria, their virulence factors, and host immunological responses interact in a complex manner, leading to irreversible tissue damage, pulp necrosis and periodontitis, a multifactorial inflammatory disease. The formation of organized, multispecies biofilms and the coordination of diverse bacterial tactics to colonize, persist, and harm periodontal tissues are important aspects of disease progression.[4]

One such factor is the adhesin protein, which mediates the adhesion and coaggregation processes between bacterial species in microbial communities. In *Fusobacterium nucleatum* bacteria, adhesin proteins such as RadD play a role in connecting the early and late stages of bacterial colonization in the dental plaque matrix.[5] The serine-rich repeat adhesin SrpA, which is produced by *Streptococcus sanguinis*, binds salivary glycoproteins and facilitates early bacterial adhesion to tooth surfaces and other microorganisms, starting the formation of biofilms.[6] To adhere to host epithelial cells, invade oral tissues, and co-aggregate with other pathogenic bacteria to sustain mature biofilms, *Porphyromonas gingivalis* utilizes FimA, a key fimbrial protein.[7]

Streptococcus mutans' D-alanine: D-alanine ligase (Ddl) is a key enzyme in the biosynthesis of peptidoglycans, preserving the integrity of the bacterial cell wall, allowing for survival in the oral cavity's acidic and immunologically demanding environment, and indirectly promoting biofilm stability by preserving bacterial viability.[8] Finally, the PLP-dependent L-cysteine desulfhydrase Cystalysin, which is secreted by *Treponema denticola*, breaks down host cysteine to produce hydrogen sulfide and ammonia. These substances harm epithelial cells, disrupt tissue barriers, and trigger inflammatory responses that contribute to the degradation of dental and surrounding oral tissues.[9]

More research is being conducted on natural substances with broad-spectrum antimicrobial activities as potential substitutes for existing antibiotics, particularly those that target bacterial virulence rather than viability. Promising candidates include phytosphingosine, arachidonic acid, trans-anethole, and eugenol, bioactive compounds that have been demonstrated antibacterial, anti-inflammatory, and biofilm-disrupting qualities.[10-13]

The structures of these compounds are presented in Figures 1. These compounds are found in Moringa oleifera, a medicinal plant traditionally used to treat systemic and oral infections.[14, 15] All the compounds were found in the extract based on the data of the extract's LC-MS analysis. The application of compounds produced from *M. oleifera* is consistent with new approaches to managing periodontitis, which seek to reduce the development of antibiotic resistance while interfering with bacterial virulence factors and biofilm formation.[16, 17]

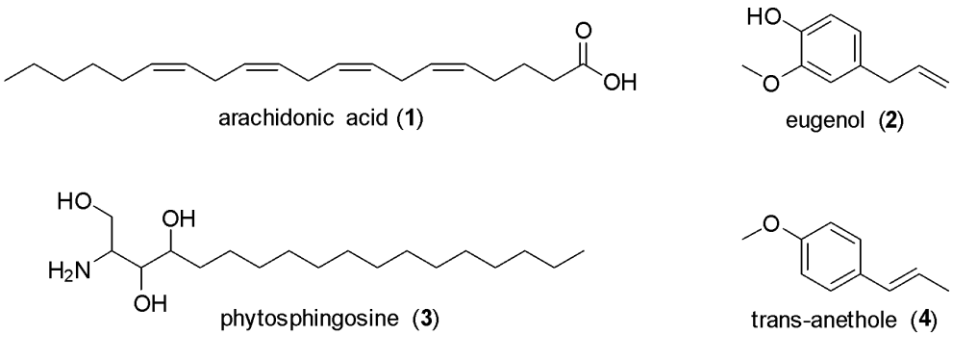

Figure 1. Structure of *Moringa oleifera* derived compounds

Comprehensive studies assessing the efficacy of natural compounds against key virulence factors involved in cariogenic and endodontic infections remain

limited, despite growing interest in these compounds as alternative antimicrobial agents. Four compounds derived from *M. oleifera*, eugenol, *trans*-anethole, arachidonic acid, and phytosphingosine, are evaluated simultaneously against a selected group of five virulence-associated proteins from major oral bacteria. These proteins of Cystalysin, FimA, Ddl, SrpA, and RadD represent various mechanisms of adhesion, biofilm formation, cell survival, and tissue destruction.

In particular, systematic in silico evaluation of several compounds derived from Moringa oleifera against key proteins that mediate adhesion, biofilm formation, bacterial survival, and tissue damage is still rare. Consequently, the comparative multi-target potential of these compounds and their mechanistic role in virulence inhibition remain poorly defined. The novelty of this study lies in the simultaneous multi-target evaluation of four *M. oleifera*–derived compounds against virulence-related proteins, an approach that has not been previously reported.

Therefore, this study aims to evaluate the interaction profiles of four Moringa oleifera–derived compounds against key virulence-associated proteins of cariogenic and endodontic pathogens using molecular docking simulations. The study further seeks to identify which compounds have the strongest potential to inhibit multiple virulence targets, providing computational evidence to support their possible use as adjuvant agents in the prevention and treatment of periodontitis.

METHODS

This study was an in silico molecular docking study conducted to evaluate compound–protein interactions using molecular docking simulations to determine the molecular activity of each compound against specified receptors. The three-dimensional structures of each receptor were obtained from the RCSB Protein Data Bank (PDB) (https://www.rcsb.org/). This study used five receptors: Cystalysin (PDB ID: 1C7O), SrpA (PDB ID: 5EQ3), FimA (PDB ID: 6JZK), RadD (PDB ID: 7R7J), and Ddl (PDB ID: 7U9K). All receptors were prepared by removing native ligands and other bound molecules before docking simulations were performed, and then saved in pdb format.

Two reference ligands were used for each target protein: the native ligand and a positive control. The native ligand refers to the biological ligand that was crystallized together with the protein in the PDB structure, representing the natural binding conformation within the active site. The positive control refers to an inhibitor or compound that has been previously reported to interact with the corresponding target protein, and is included to provide a reference for comparison with the docking performance of the tested phytochemical compounds. L-arginine for RadD, D-glycoserine for Cystalisin and Ddl, Neu5Gc for SrpA and GalNAc for FimA were the three positive controls utilized in this study. All structures were obtained from PubChem (CIDs: 67427, 440001, 6234, and 35717). Four compounds (arachidonic acid, eugenol, phytosphingosine, and *trans*-anethole) derived from *M. oleifera* were examined for their capacity to interfere with virulence factors of periodontitis.

The structures of arachidonic acid, eugenol, phytosphingosine, and *trans*-anethole were obtained from the PubChem website (https://pubchem.ncbi.nlm.nih.gov/) with CIDs of 444899, 3314, 122121, and 637563, respectively. After downloading each ligand structure in SDF format, all structures were converted to PDB format and optimized using Chem3D Ultra 12.0's MM2 energy minimizer, and saved in pdb format

To validate the docking protocol, each native ligand was re-docked to its respective protein binding site following receptor and ligand preparation. AutoDock 4.0 was used to perform molecular docking simulations. Each receptor and ligand in PDB format was converted to PDBQT format before the simulation

began. For each receptor, a grid box measuring 40 Å x 40 Å x 40 Å was applied, with specific x, y, and z coordinates for the grid center. The root mean square deviation (RMSD) between the docking pose and the crystallographic pose was calculated to assess the reliability of the docking setup.

RMSD values < 3.0 Å were considered acceptable, indicating that the selected docking parameters were able to accurately reproduce the experimentally observed bond conformations. Re-docking conformations were visualized using Discovery Studio 2024 software.

The compound docking process was performed using AutoDock 4.0 software, similar to the re-docking procedure. The bond energy and inhibition constant for each receptor-ligand complex were obtained from the test results, and the receptor-ligand interactions were analyzed and visualized using Discovery Studio 2024. Graphs were generated to illustrate hydrophobic interactions and hydrogen bonding within receptor-ligand complexes.

RESULTS

Before evaluating the interactions of Moringa oleifera–derived compounds with target proteins, the docking protocol was first validated to ensure reliability. Re-docking of native ligands into their respective binding sites was performed, and the resulting root mean square deviation (RMSD) values were assessed. The re-docking RMSD values and conformations are presented in Table 1 and Figure 2.

Table 1. Grid center coordinates for each receptor

+name	PDB ID	Positive Control	Grid Center (coordinates)			RMSD
			x	y	z	
Cystalysin	1C7O	D-glycoserine	14.561	-4.847	20.75	2.167
SrpA	5EQ3	Neu5Gc	15.260	11.538	9.568	2.436
FimA	6JZK	GalNAc	1.287	-3.755	93.097	3.102
RadD	7R7J	L-Arginine	-6.627	-37.876	107.279	3.097
Ddl	7U9K	D-glycoserine	7.923	20.387	27.732	1.159

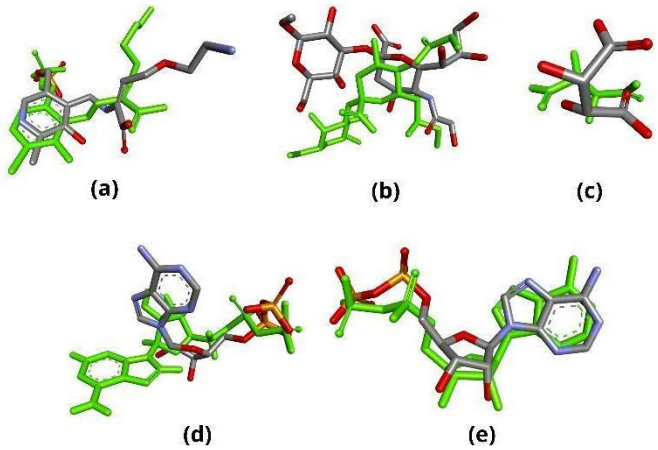

Figure 2. Re-docking conformation for a. Cystalysin, b. SrpA, c. FimA, d. RadD, and e. Ddl.

The molecular docking interactions between *Moringa oleifera*–derived compounds and bacterial virulence target proteins are presented in Table 2. The parameters analyzed included binding free energy (ΔG), inhibition constant (Ki), amino acid residues involved in hydrogen bonding, and hydrophobic interactions that contribute to the stability of the ligand-receptor complex. Comparisons were made between test compounds, native ligands, and positive controls to evaluate relative binding affinity and potential biological activity. These results provide a basis for identifying compounds with the best affinity for target proteins involved in cariogenic processes and endodontic infections.

Table 2. Molecular docking summary for all ligand–target pairs

Target	Ligand	ΔG	Ki	hydrogen bonds	hydrophobic interactions
Cystalysin	Native	-6.78	10.76	Val98, Ala243, Tyr123, Ser237, Cys171, Lys238	-
	Positive control	-5.21	150.55	Arg369, Tyr124, Asp355, Ala39	-
	Comp. (1)	-5.13	174.80	Lys238, Tyr123	Cys171, Val99, Val98, Ala39, His206, Ile205, Val38, Ala243
	Comp. (2)	-5.64	72.98	Lys238, Tyr123, His206	Ala39, Ile205
	Comp. (3)	-3.81	1620	Ala39, Tyr123, Tyr124	Val99, Val98, Ile205, His206, Lys238, Ala235
	Comp. (4)	-5.17	161.76	Ala39, Tyr123, Asp355, Tyr124	Ala39, Cys171, Ile205, His206
SrpA	Native	-6.36	21.70	Thr346, Gln344, Pro335, Tyr368, Arg347	Pro337, Arg342
	Positive control	-5.82	53.74	Arg342, Arg347, Thr346, Gln344, Tyr368, Ala343	-
	Comp. (1)	-1.73	54.29×10^3	Arg342	Pro337, Phe294
	Comp. (2)	-4.22	802.41	Arg347, Thr346	Phe345, Gln344
	Comp. (3)	-3.18	4.663×10^3	Gln344, Arg347,Thr346	Phe345, Pro347, Arg342
	Comp. (4)	-3.78	1.69×10^3	Thr346	Arg342, Gln344
FimA	Native	-4.96	230.57	Lys59, Thr61, Ser75, Met103	-
	Positive control	-4.73	343.084	Gly101, Ala102, Met103, Leu105, Val106	-
	Comp. (1)	-3.97	1230	Lys59, Ser75	Lys108, Val106, Leu105
	Comp. (2)	-4.19	843.62	Met103	Ile73, Leu105
	Comp. (3)	-1.74	53.30×10^3	Glu104, Val106	Ile73, Leu105
	Comp. (4)	-4.04	1090	Ser75	Leu105, Val106, Ile73
RadD	Native	-8.27	0.89×10^{-3}	Arg343, Arg6, Tyr195, Gly36, Gly34, Ala35, Thr33	Arg343, Leu344
	Positive control	-2.78	9230	Asp315, Tyr195, Gly34, Arg6	-
	Comp. (1)	-4.65	390.63	Lys37, Thr33	Lys68, Arg6, Leu39, Leu72
	Comp. (2)	-4.00	1170	Gly36, Lys37	Ala35
	Comp. (3)	-2.67	11.12×10^3	Gly34, Arg6, Tyr195, Leu344	Leu39, Leu72, Ala71, Lys37, Lys68
	Comp. (4)	-4.42	579.42	Gly34, Pro32	Leu39, Leu72, Lys68, Lys37, Ala35
DdI	Native	-8.94	0.28×10^{-3}	Lys130, Asn305, Glu213, Val216, Gln214, Glu220, Tyr246, Ser184, Gly182, Asn308, Ser183, Lys251	-
	Positive control	-6.09	34.60	Ile221, Phe294, Asn305, Glu222	-
	Comp. (1)	-6.52	16.49	Asn305	Leu145, Val216, Phe295, Phe175, Phe245, Ile187
	Comp. (2)	-5.40	109.80	Ala218, Ala244, Glu220	Phe295, Phe175, Leu145
	Comp. (3)	-7.42	3.61	Glu222, Arg291, Glu306, Asp293, Lys251	Phe295, Phe245, Phe175, Leu145
	Comp. (4)	-5.25	142.83	Phe245, Tyr246	Phe175, Phe295, Leu145

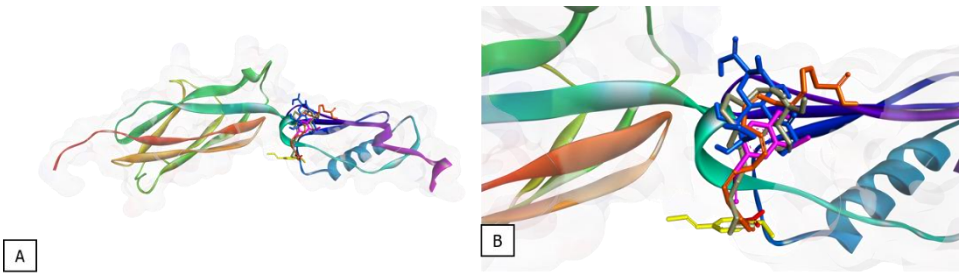

Figure 3. Conformations of the native ligand, *M. oleifera* compounds, and positive controls at SrpA A, ligand conformational positioning receptor, and B. close-up view.

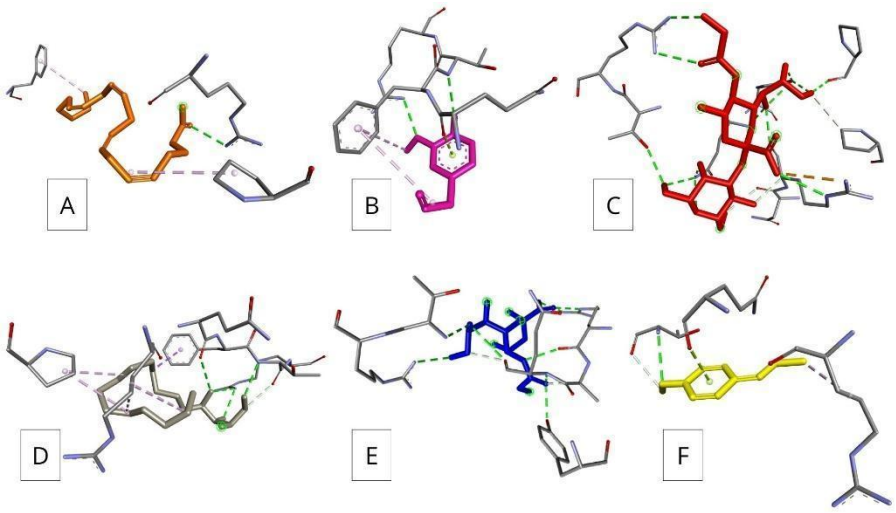

Figure 4. Molecular interactions of SrpA receptor with A. Arachidonic acid, B. eugenol, C.native ligand, D. phytosphingosine, E. positive control, and F. *trans*-anethole.

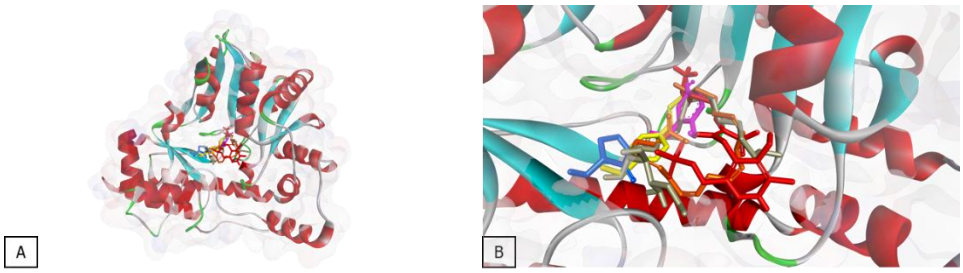

Figure 5. Conformations of the native ligand, *M. oleifera* compounds, and positive controls at Cystalysin A, ligand conformational positioning receptor, and B. Close-up view.

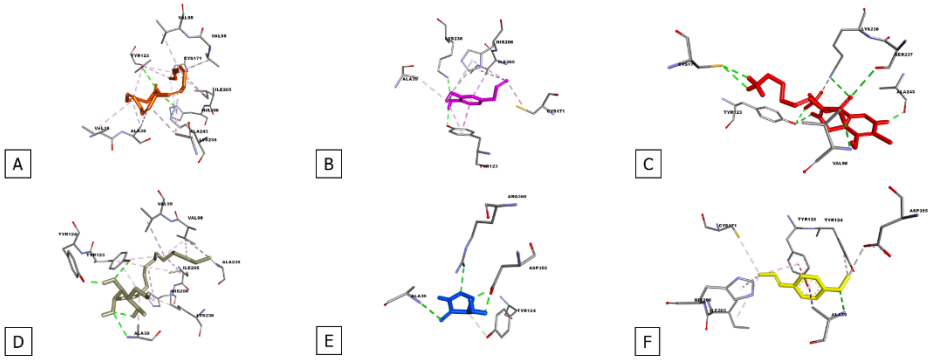

Figure 6. Molecular interactions of Cystalysin receptor with A. Arachidonic acid, B. eugenol, C. native ligand, D. phytosphingosine, E. positive control, and F. *trans*-anethole.

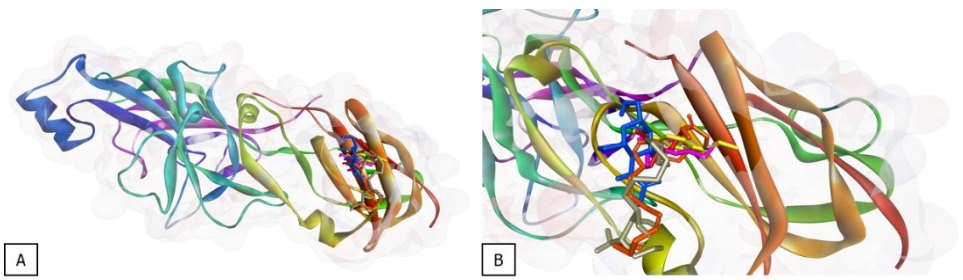

Figure 7. Conformations of the native ligand, *M. oleifera* compounds, and positive controls at FimA A, ligand conformational positioning receptor, and B. Close-up view.

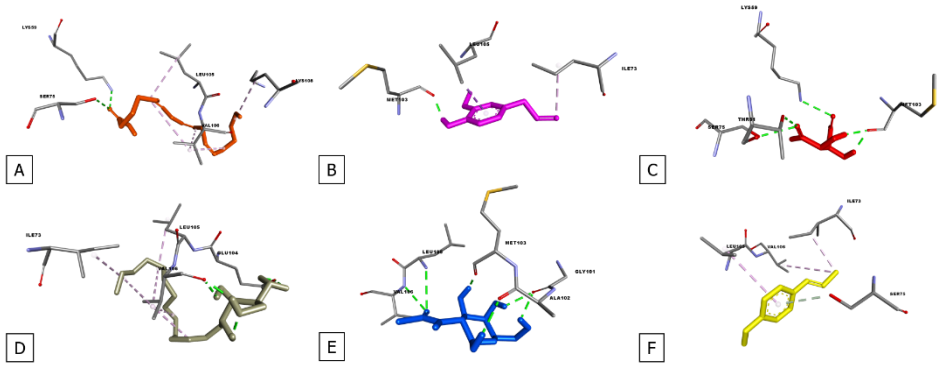

Figure 8. Molecular interactions of FimA receptor with A. Arachidonic acid, B. eugenol, C. native ligand, D. phytosphingosine, E. positive control, and F. *trans*-anethole

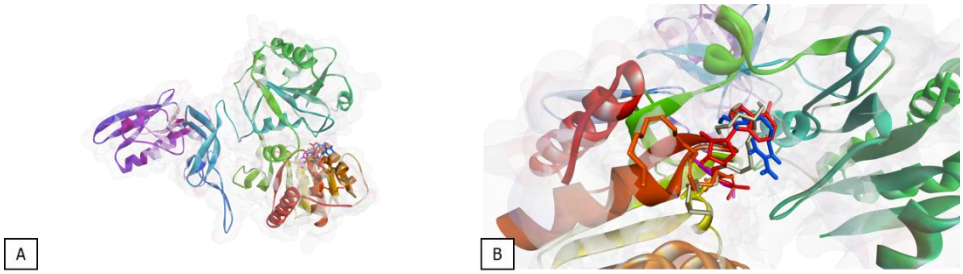

Figure 9. Conformations of the native ligand, *M. oleifera* compounds, and positive controls at RadD A, ligand conformational positioning receptor, and B Close-up view.

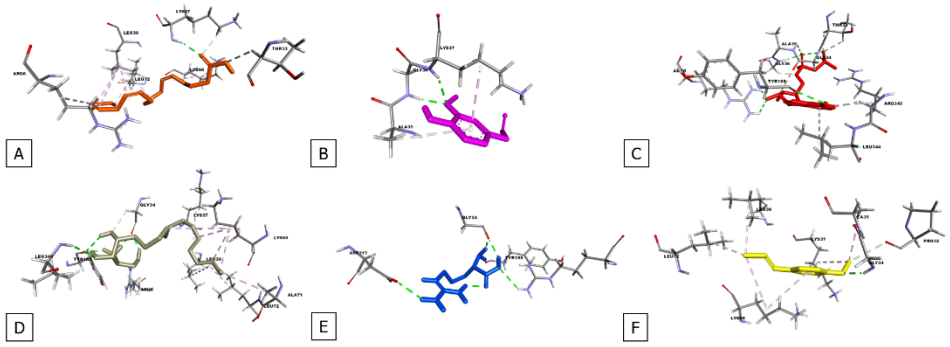

Figure 10. Molecular interactions of RadD receptor with A. Arachidonic acid, B. eugenol, C. native ligand, D. phytosphingosine, E. positive control, and F. *trans*-anethole.

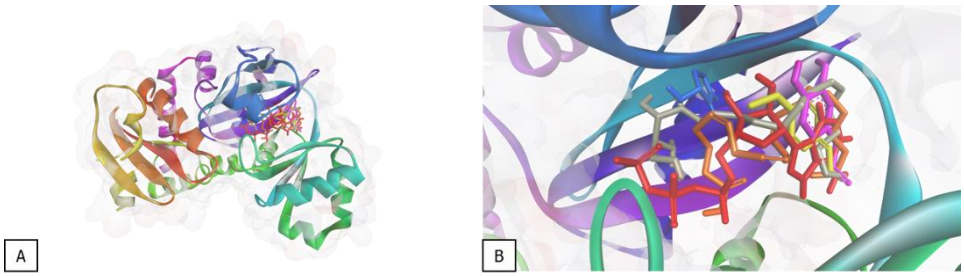

Figure 11. Conformations of the native ligand, *M. oleifera* compounds, and positive controls at Ddl A, ligand conformational positioning receptor, and B. Close-up view.

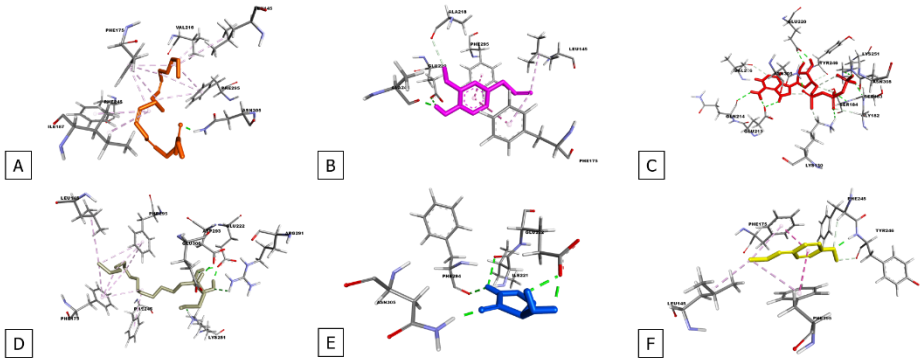

Figure 12. Molecular interactions of Ddl receptor with A. Arachidonic acid, B. eugenol, C. native ligand, D. phytosphingosine, E. positive control, and F. *trans*-anethole.

DISCUSSION

This study explores *Moringa oleifera*-derived compounds as potential multi-target inhibitors of key proteins involved in various stages of cariogenic and endodontic pathogenesis. Previous studies have reported that *M. oleifera* possesses antibacterial and anti-biofilm activities against oral pathogens, primarily attributed to its rich phytochemical content, including phenolics and fatty acids.[18] Molecular docking, along with detailed analysis of hydrogen bonding and hydrophobic interactions, was performed to determine how these compounds might interfere with adhesion-related receptors, enzymes required for bacterial survival, and factors involved in host tissue damage. The results offer new insights into the ability of *M. oleifera* compounds to disrupt multiple virulence mechanisms relevant to dental infection progression, highlighting their potential as supplementary agents in comprehensive conservative dental therapy.[18, 19]

The interaction potential of four compounds derived from *Moringa oleifera* extract against key virulence-associated proteins of cariogenic and endodontic pathogens was evaluated using molecular docking simulations. Scoring functions are used by docking programs to estimate binding energy.[20] The four compounds derived from *M. oleifera* showed different affinities for the five target proteins according to molecular docking simulations. The lowest (i.e., strongest) binding energies were typically displayed by the native ligands, with RadD (-8.27 kcal/mol) and Ddl (-8.94 kcal/mol) being especially notable. Eugenol showed consistently favorable binding energies across the majority of targets among the investigated natural compounds (-5.64 to -3.46 kcal/mol), followed by *trans*-anethole (-5.17 to -3.61 kcal/mol) and arachidonic acid (-5.13 to -1.73 kcal/mol).

The weakest binding affinity was observed for phytosphingosine, particularly with FimA (-1.74 kcal/mol) and SrpA (-2.68 kcal/mol), indicating a low interaction strength with these adhesin targets. Positive controls demonstrated varied binding, with RadD (-2.78 kcal/mol) showing least favorably and Ddl (-6.09 kcal/mol) performing the best. A similar trend was observed in the calculated inhibition constants (Ki). Across all targets, the compounds showed Ki values in the nanomolar to millimolar range; native ligand binding to RadD (0.89 $x10^{-3}$ µM or 890 nM) and Ddl (0.28 $x10^{-3}$ µM) had the lowest (strongest) Ki values, supporting their role as reference benchmarks for evaluating ligand performance.

These findings are consistent with previous docking studies, where binding energies stronger than -6.0 kcal/mol are generally considered indicative of moderate to strong ligand-protein interactions, particularly for enzymatic targets such as D-alanine:D-alanine ligase, whereas weaker interactions (above -4.0 kcal/mol) are typically associated with low binding stability or nonspecific interactions.[22]

A similar trend was observed in the calculated inhibition constants (Ki), which ranged from nanomolar to millimolar levels across all targets. The native ligands for RadD (0.89×10^{-3} µM, equivalent to 890 nM) and Ddl (0.28×10^{-3} µM) exhibited the lowest Ki values, reflecting their high binding affinity and biological

relevance. These results are in agreement with previous reports indicating that biologically active ligands typically display Ki values in the nanomolar to low micromolar range, while weaker inhibitors fall into the higher micromolar to millimolar range.[23]

However, the Ki values of the compounds were higher (weaker) than those of their respective positive controls for a number of targets, particularly SrpA and FimA. $54.29x10^3$ µM or 54.29 mM for arachidonic acid binding to SrpA and $53.30x10^3$ µM for phytosphingosine binding to FimA. This variation may be attributed to differences in how scoring functions account for hydrophobic and hydrogen bonding interactions. Higher binding affinities are generally indicated by lower (more negative) binding energies, which also imply a more stable and favorable interactions.[21, 22] According to the docking data, almost all test ligands form 2–4 hydrogen bonds, mainly with key residues such as Lys238, Tyr123, His206, Ala39, and Val99. These residues are part of the same binding pocket as the native ligand, so the interaction of the test ligand can be said to overlap with the physiological binding site. This overlap indicates that the ligand is able to inhibit the proteolytic activity of Cystalysin (figure 5-6) through direct competition with the natural ligand. The greater the number of H-bonds, the more stable the interaction, and this is consistent with the relatively low ΔG and Ki values.[19]

In SrpA (figure 3-4), the test ligands generally form 1–3 H-bonds, with important residues such as Lys340, Lys373, Asp434, Thr372, which are known to be located in the sialic-acid–binding groove of SrpA. Previous structural studies have demonstrated that these residues play a critical role in recognizing and stabilizing sialic acid during bacterial adhesion, particularly through electrostatic and hydrogen-bond interactions.[26] The interaction of the test ligands with these residues indicates that they occupy a similar binding region as the native sialic acid ligand, suggesting a competitive binding mode. This finding is consistent with earlier docking and crystallographic studies, where ligands capable of interacting with key lysine and aspartate residues exhibited effective inhibition of sialoglycan binding.[27]

Furthermore, ligands with lower binding free energy (ΔG), such as Compound 3 and Compound 4, showed a higher degree of overlap with the native ligand binding site, supporting their potential as competitive inhibitors of SrpAsialoglycan adhesion. Ligands to FimA (figure 7-8) show the formation of 2–3 H-bonds with residues such as Lys59, Ser75, Glu70, Val105, which are residues corresponding to the native ligand interaction site. These findings are in agreement with previous studies indicating that polar and charged residues in the FimA binding pocket are essential for ligand recognition and stabilization.[28]

The overlap between the test ligand interactions and the native binding site suggests a competitive inhibition mechanism, where the ligands may block the adhesion process by occupying the functional binding pocket.[29] Similar interaction patterns have been reported in other adhesin-targeted docking studies, where hydrogen bonding with key residues contributes significantly to binding specificity. In addition to hydrogen bonding, hydrophobic interactions involving residues such as Leu104 and Ile73 further enhance complex stability, which is consistent with previous reports highlighting the importance of hydrophobic contacts in maintaining ligand-protein interactions within adhesin domains.

In RadD (figure 9-10), the ligands exhibited a similar interaction pattern, forming 1-3 hydrogen bonds primarily with residues such as Gly36, Arg45, Tyr195, and Lys73, which are located within the predicted interaction domain of the protein. Previous studies have shown that RadD functions as an adhesin involved in interspecies bacterial aggregation, where charged residues such as arginine and lysine play a crucial role in mediating electrostatic interactions with partner cells.[30]

The interaction of the test ligands with Arg45 and Lys73 suggests that these compounds occupy regions critical for adhesion-related interactions, indicating a potential competitive binding mechanism. This observation is consistent with prior

computational and functional studies, where ligands targeting positively charged residues in adhesin domains were able to disrupt protein-protein interactions.

Furthermore, ligands with more negative binding free energy (ΔG) values demonstrated a greater degree of overlap with the predicted interaction interface, supporting their potential to competitively interfere with the RadD-mediated adhesion mechanism.[31] In Ddl (figure 11-12), the ligands formed 2-4 hydrogen bonds with key active-site residues, including Glu223, Asp293, Lys251, and Phe295. These residues are well documented as part of the catalytic pocket responsible for D-alanine activation and D-Ala-D-Ala dipeptide formation, a crucial step in bacterial peptidoglycan biosynthesis.[32]

The interaction of the test ligands with Glu223 and Lys251 is particularly significant, as these residues are directly involved in substrate binding and catalytic activity. Previous structural and inhibition studies have shown that compounds interacting with these residues can effectively block the enzymatic formation of D-Ala-D-Ala, thereby inhibiting bacterial cell wall synthesis.[33]

The observed overlap between the test ligands and the native substrate binding site indicates a competitive inhibition mechanism. Moreover, ligands exhibiting lower ΔG values showed stronger and more stable interactions within the catalytic pocket, further supporting their potential as Ddl inhibitors, consistent with earlier docking and enzymatic inhibition studies.

The complexes stabilized ligand–receptor binding in active or binding sites by forming numerous hydrogen bonds across several targets with important catalytic or binding-site residues.[34] Lower (larger) binding energies and maybe stronger inhibitory effects are the outcome of compounds that can form hydrogen bonds. These compounds are thus more likely to stay anchored inside the active site. For instance, eugenol formed hydrogen bonds with Lys238 and Tyr123 in Cystalysin, important catalytic residues essential for PLP-dependent activity.

These interactions suggest a potential disruption of enzymatic function. Phytosphingosine presented the most hydrogen bonds compared to the other compounds, which generated an extensive hydrogen bond complex. Hydrogen bond networks consist of interactions connecting the side chains of numerous residues throughout the protein. Hydrogen bond networks stabilize the overall protein structure and have been shown to play a role in activation and allostery.[35] Eugenol also exhibited strong hydrogen bonding interactions, as indicated by the number of hydrogen bonds formed.

These polar interactions imply that these substances can successfully stabilize their binding to vital virulence proteins, which may interfere with the mechanisms of bacterial colonization or survival.[36] The conformations of all the ligands were illustrated in Figures 3, 5, 7, 19, and 11 followed by the molecular interactions of hydrogen bonds and hydrophobic interactions for each ligand in a specific receptor were demonstrated in Figures 4, 6, 9, 10, and 12. Ligands are color-coded for clarity: red (native ligand), blue (positive control), orange (arachidonic acid), purple (eugenol), grey (phytosphingosine), and yellow (trans-anethole).

Hydrophobic interactions, primarily driven by van der Waals forces with nonpolar residues, play an important role in stabilizing ligand-protein complexes. Previous studies have shown that hydrophobic contacts significantly contribute to binding affinity, especially when combined with hydrogen bonding. [37] In this study, phytosphingosine and arachidonic acid exhibited the most frequent hydrophobic interactions across targets, involving residues such as Phe295 and Leu145 in Ddl, Ile73 and Leu105 in FimA, and Ala39 and Ile205 in Cystalysin. Similar patterns have been reported, where residues like leucine, isoleucine, and phenylalanine play key roles in ligand stabilization.[38, 39]

However, despite extensive hydrophobic interactions, phytosphingosine showed relatively weak binding affinity, indicating that hydrophobic contacts alone are insufficient without complementary hydrogen bonding and electrostatic interactions. These interactions are particularly important for lipophilic

compounds, which rely on embedding within hydrophobic pockets to achieve effective binding. The moderate to strong binding energies observed for these compounds may be attributed to extensive hydrophobic interactions, sometimes complemented by hydrogen bonding. This supports the compounds' potential as multi-target inhibitors of oral bacterial virulence factors.[40]

The limitation of this study is that the findings are based solely on in silico molecular docking simulations, which may not fully represent the complexity of biological systems. Docking scores and predicted binding modes do not account for pharmacokinetic properties, compound solubility, membrane permeability, or metabolic stability, which may influence biological activity in vivo. Furthermore, protein flexibility and solvent effects were only partially considered, which may affect the accuracy of predicted ligand-receptor interactions. Therefore, the inhibitory potential of the investigated compounds should be interpreted as preliminary and hypothesis-generating rather than definitive evidence of biological efficacy.

CONCLUSION

This in silico molecular docking study demonstrated that Moringa oleifera–derived compounds, particularly phytosphingosine, exhibit strong binding affinity toward key virulence-associated proteins of cariogenic and endodontic pathogens. These findings highlight the potential of M. oleifera as a natural source of antibacterial agents; however, further in vitro and in vivo studies are required to validate these findings.

The implications of this research suggest that *M. oleifera*-derived compounds could serve as promising lead molecules for the development of multi-target antibacterial agents and adjunctive therapeutics in conservative dental therapy, particularly for managing complex cariogenic and endodontic infections.

Acknowledgement: The authors would like to express their sincere gratitude to Universitas Trisakti for providing the facilities and support that enabled the completion of this research.
Author Contributions: Conceptualization, MFA, DK,TA, DH; methodology, MFA, DK, TA, DH; software, DK, DH ; validation, MFA, DK, TA, DH ; formal analysis, MFA, DK, TA, DH ; investigation, MFA, DK, TA, DH ; resources, MFA, DK, TA, DH ; data curation, DK, DH; writing original draft preparation, MFA, DK, TA, DH; writing review and editing, MFA, DK, TA, DH; visualization, DK, DH; supervision, MFA, DK, TA, DH; All authors have read and agreed to the published version of the manuscript.
Funding: No funding was received for this study.
Institutional Review Board Statement: Ethical approval was waived because the study does not involve human subjects or animal experiments.
Informed Consent Statement: Not applicable.
Data Availability Statement: The data used to support the findings of this study are included within the article. Raw data that support the findings of this study are available from the author, upon reasonable request.
Conflicts of Interest: The authors declare no conflict of interest.

REFERENCES

1. Könönen E, Gursoy M, Gursoy UK. Periodontitis: a multifaceted disease of tooth-supporting tissues. J Clin Med. 2019;8(8):1135. https://doi.org/10.3390/jcm8081135
2. Giambartolomei GH, Delpino MV. Immunopathogenesis of hepatic brucellosis. Front Cell Infect Microbiol. 2019;9:423. https://doi.org/10.3389/fcimb.2019.00423
3. Kwon T, Lamster IB, Levin L. Current concepts in the management of periodontitis. Int Dent J. 2021;71(6):462–476. https://doi.org/10.1111/idj.12630
4. Miller DP. Microbial biofilms and pathobiology of gingivitis and periodontitis. In: Oral Biofilms in Health and Disease. Cham: Springer; 2025. p. 275–309. https://doi.org/10.1007/978-3-031-82202-510
5. GC B, Wu C. The CarSR two-component system directly controls radD expression as a global regulator that senses bacterial coaggregation in Fusobacterium nucleatum. J Bacteriol. 2025;207(6):e00529-24. https://doi.org/10.1128/jb.00529-24
6. Zhu F, Zhang H, Yang T, Haslam SM, Dell A, Wu H. Engineering and dissecting the glycosylation pathway of a streptococcal serine-rich repeat adhesion. J Biol Chem. 2018;293(13):4952–4963. https://doi.org/10.1074/jbc.AAC118.002681
7. Hasegawa Y, Nagano K. Porphyromonas gingivalis FimA and Mfa1 fimbriae: current insights on localization, function, biogenesis, and genotype. Jpn Dent Sci Rev. 2021;57:190–200. https://doi.org/10.1016/j.jdsr.2021.09.003
8. Batson S, de Chiara C, Majce V, Lloyd AJ, Gobec S, Rea D, et al. Inhibition of D-Ala:D-Ala ligase through a phosphorylated form of the antibiotic D-cycloserine. Nat Commun. 2017;8(1):1939. https://doi.org/10.1038/s41467-017-02118-7

9. Şenel S. An overview of physical, microbiological and immune barriers of oral mucosa. Int J Mol Sci. 2021;22(15):7821. https://doi.org/10.3390/ijms22157821
10. Elbestawy MK, El-Sherbiny GM, Moghannem SA. Antibacterial, antibiofilm and anti-inflammatory activities of eugenol clove essential oil against resistant Helicobacter pylori. Molecules. 2023;28(6):2448. https://doi.org/10.3390/molecules28062448
11. Chamlagain M, Hu J, Sionov RV, Steinberg D. Anti-bacterial and anti-biofilm activities of arachidonic acid against the cariogenic bacterium Streptococcus mutans. Front Microbiol. 2024;15:1333274. https://doi.org/10.3389/fmicb.2024.1333274
12. Glenz R, Kaiping A, Göpfert D, Weber H, Lambour B, Sylvester M, et al. The major plant sphingolipid long-chain base phytosphingosine inhibits growth of bacterial and fungal plant pathogens. Sci Rep. 2022;12(1):1081. https://doi.org/10.1038/s41598-022-05083-4
13. Medeiros M, Alves M, Santos B, Silva E, Araújo F, Bezerra M, et al. Evaluation of the antibacterial activity of trans-anethole against Enterococcus cloacae and Enterococcus faecalis strains of food origin. Braz J Biol. 2023;83:e269245. https://doi.org/10.1590/1519-6984.269245
14. Dixit K, Chauhan B, Jain R. Anti-inflammatory potential of medicinal plants in the management of inflammatory diseases: a review of mechanisms and bioactive compounds. J Drug Deliv Ther. 2025;15(6). https://doi.org/10.22270/jddt.v15i6.7203
15. Ojewumi ME, Obanla OR, Atauba DM. A review on the efficacy of Ocimum gratissimum, Mentha spicata, and Moringa oleifera leaf extracts in repelling mosquito. Beni-Suef Univ J Basic Appl Sci. 2021;10(1):87. https://doi.org/10.1186/s43088-021-00176-x
16. Jaya FB, Syamsunarno MRAA, Sahiratmadja E. Moringa oleifera Lam. to accelerate wound healing: a review. Berkala Ilmu Kedokteran. 2023;55(3). https://doi.org/10.19106/JMedSci005503202310
17. Baky NAA, Fouad LM, Ahmed KA, Alzokaky AA. Mechanistic insight into the hepatoprotective effect of Moringa oleifera Lam leaf extract and telmisartan against carbon tetrachloride-induced liver fibrosis. Drug Chem Toxicol. 2025;48(1):84–97. https://doi.org/10.1080/01480545.2024.2358066
18. Vergara-Jimenez M, Almatrafi MM, Fernandez ML. Bioactive components in Moringa oleifera leaves protect against chronic disease. Antioxidants. 2017;6(4):91. https://doi.org/10.3390/antiox6040091
19. Yasir M, Park J, Han ET, Han JH, Park WS, Choe J, et al. Identification of marine compounds inhibiting NF-κB-inducing kinase through molecular docking and molecular dynamics simulations. Biomolecules. 2024;14(12):1490. https://doi.org/10.3390/biom14121490
20. Vikhar DA, Khan SW, Ali SA, Yasar Q. Network pharmacology combined with molecular docking and experimental verification to elucidate the effect of flavan-3-ols and aromatic resin on anxiety. Sci Rep. 2024;14(1):9799. https://doi.org/10.1038/s41598-024-58877-z
21. Fattouche M. Multi-combined drug-likeness, 3D-QSAR modeling, molecular docking and molecular dynamics analysis of several series of pharmaceutical compounds [dissertation]. Biskra: Université Mohamed Khider; 2024.
22. Meng XY, Zhang HX, Mezei M, Cui M. Molecular docking: a powerful approach for structure-based drug discovery. Curr Comput Aided Drug Des. 2011;7(2):146–157. https://doi.org/10.2174/157340911795677602
23. Gilson MK, Zhou HX. Calculation of protein–ligand binding affinities. Annu Rev Biophys Biomol Struct. 2007;36(1):21–42. https://doi.org/10.1146/annurev.biophys.36.040306.132550
24. Zothantluanga JH, Chetia D. A beginner's guide to molecular docking. Sci Phytochem. 2022;1(2):90–93. https://doi.org/10.58920/sciphy01020037
25. Pantsar T, Poso A. Binding affinity via docking: fact and fiction. Molecules. 2018;23(8):1899. https://doi.org/10.3390/molecules23081899
26. Plummer C, Wu H, Kerrigan SW, Meade G, Cox D, Ian Douglas CW. A serine-rich glycoprotein of Streptococcus sanguis mediates adhesion to platelets via GPIb. Br J Haematol. 2005;129(1):101–109. https://doi.org/10.1111/j.1365-2141.2005.05421.x
27. Buchanan CJ, Gaunt B, Harrison PJ, Yang Y, Liu J, Khan A, et al. Pathogen-sugar interactions revealed by universal saturation transfer analysis. Science. 2022;377(6604):eabm3125. https://doi.org/10.1126/science.abm3125
28. Mishra A, Devarajan B, Reardon ME, Dwivedi P, Krishnan V, Cisar JO, et al. Two autonomous structural modules in the fimbrial shaft adhesin FimA mediate Actinomyces interactions with streptococci and host cells during oral biofilm development. Mol Microbiol. 2011;81(5):1205–1220. https://doi.org/10.1111/j.1365-2958.2011.07745.x
29. Skolnick J, Zhou H. Implications of the essential role of small molecule ligand binding pockets in protein–protein interactions. J Phys Chem B. 2022;126(36):6853–6867. https://doi.org/10.1021/acs.jpcb.2c04525
30. Kaplan CW, Lux R, Haake SK, Shi W. The Fusobacterium nucleatum outer membrane protein RadD is an arginine-inhibitable adhesin required for inter-species adherence and the structured architecture of multispecies biofilm. Mol Microbiol. 2009;71(1):35–47. https://doi.org/10.1111/j.1365-2958.2008.06503.x
31. Komarov IV, Bugrov VA, Cherednychenko A, Grygorenko OO. Insights into modeling approaches in chemistry: assessing ligand–protein binding thermodynamics based on rigid–flexible model molecules. Chem Rec. 2024;24(2):e202300276. https://doi.org/10.1002/tcr.202300276
32. Qin Y, Xu L, Teng Y, Wang Y, Ma P. Discovery of novel antibacterial agents: recent developments in D-alanyl-D-alanine ligase inhibitors. Chem Biol Drug Des. 2021;98(3):305–322. https://doi.org/10.1111/cbdd.13899
33. Nocentini A. D-alanine–D-alanine ligase. In: Metalloenzymes. 2024. p. 83–91. https://doi.org/10.1016/B978-0-12-823974-2.00009-7
34. Chen D, Oezguen N, Urvil P, Ferguson C, Dann SM, Savidge TC. Regulation of protein–ligand binding affinity by hydrogen bond pairing. Sci Adv. 2016;2(3):e1501240. https://doi.org/10.1126/sciadv.1501240
35. Bertalan É, Lešnik S, Bren U, Bondar AN. Protein–water hydrogen-bond networks of G protein-coupled receptors. J Struct Biol. 2020;212(3):107634. https://doi.org/10.1016/j.jsb.2020.107634
36. Zhao G, Liu X, Wang S, Bai Z, Zhang S, Wang Y, et al. Hydrogen bonding penalty used for virtual screening to discover potent inhibitors for papain-like cysteine proteases of SARS-CoV-2. Chem Biol Drug Des. 2022;100(4):502–514. https://doi.org/10.1111/cbdd.14115

37. Kawatkar SP, Keating TA, Olivier NB, Breen JN, Green OM, Guler SY, et al. Antibacterial inhibitors of gram-positive thymidylate kinase: structure–activity relationships and chiral preference of a new hydrophobic binding region. J Med Chem. 2014;57(11):4584–4597. https://doi.org/10.1021/jm500463c
38. Bitencourt-Ferreira G, Veit-Acosta M, de Azevedo WF Jr. Van der Waals potential in protein complexes. In: Docking Screens for Drug Discovery. Cham: Springer; 2019. p. 79–91. https://doi.org/10.1007/978-1-4939-9752-7_6
39. Li J, Ma X, Guo S, Hou C, Shi L, Zhang H, et al. A hydrophobic-interaction-based mechanism triggers docking between the SARS-CoV-2 spike and angiotensin-converting enzyme 2. Glob Chall. 2020;4(12):2000067. https://doi.org/10.1002/gch2.202000067
40. Du X, Li Y, Xia YL, Ai SM, Liang J, Sang P, et al. Insights into protein–ligand interactions: mechanisms, models, and methods. Int J Mol Sci. 2016;17(2):144. https://doi.org/10.3390/ijms17020144

https://doi.org/10.24198/pjd.vol38no1.68102 Submitted to Padjadjaran Journal of Dentistry for possible open access publication under the terms and conditions of the Creative Commons Attribution (CC BY-NC 4.0) license https://creativecommons.org/licenses/by-nc/4.0/